

Tree-rings and the climate of New Caledonia (SW pacific) preliminary results from Araucariaceae

Vincent Lieubeau, Pierre Genthon, M. Stievenard, R. Nasi, Valérie
Masson-Delmotte

► **To cite this version:**

Vincent Lieubeau, Pierre Genthon, M. Stievenard, R. Nasi, Valérie Masson-Delmotte. Tree-rings and the climate of New Caledonia (SW pacific) preliminary results from Araucariaceae. *Palaeogeography, Palaeoclimatology, Palaeoecology*, Elsevier, 2007, 253 (3-4), pp.477-489. <10.1016/j.palaeo.2007.06.019>. <ird-00310138>

HAL Id: ird-00310138

<http://hal.ird.fr/ird-00310138>

Submitted on 7 Aug 2008

HAL is a multi-disciplinary open access archive for the deposit and dissemination of scientific research documents, whether they are published or not. The documents may come from teaching and research institutions in France or abroad, or from public or private research centers.

L'archive ouverte pluridisciplinaire **HAL**, est destinée au dépôt et à la diffusion de documents scientifiques de niveau recherche, publiés ou non, émanant des établissements d'enseignement et de recherche français ou étrangers, des laboratoires publics ou privés.

1 Tree-rings and the climate of New Caledonia (SW Pacific).

2 Preliminary results from Araucariaceae.

3

4 Lieubeau Vincent⁽¹⁾, Genthon Pierre^(1,*), Stievenard Michel⁽³⁾, Nasi Robert⁽²⁾,

5 Masson-Delmotte, Valérie⁽³⁾

6

7 ¹ IRD Paléotropique Noumea BP A5 98848 Noumea New Caledonia

8 ² CIFOR/CIRAD , TA 10/D 34398 Montpellier France

9 ³ Laboratoire des Sciences du Climat et de l'Environnement, IPSL/CEA-CNRS Gif/Yvette

10 France.

11 * corresponding author at genthon@msem.univ-montp2.fr, fax: 334 67 14 74 47

12

13

14

15 **Abstract**

16

17 The dendroclimatologic potential of some Araucariaceae of New Caledonia (including *Agathis*, or
18 *kauris*, and *Araucaria*) is assessed using ring thickness and $\delta^{18}\text{O}$ measurements. New Caledonia is a
19 group of islands in the SW Pacific that are currently under influence of ENSO events. Endemic to
20 New Caledonia, the long-living species of *Agathis lanceolata* and *A. ovata*, growing on poor
21 ultramafic-derived soils may provide valuable proxies for the local climate and for ENSO. These trees
22 present visible growth bands of changing thickness along their circumference. However, several bands
23 are locally absent, and the growth axis is generally offset with respect to the geometrical axis of the
24 tree. This led us to compute so-called composite ring thickness profiles, accounting for the geometry
25 of growth bands on the whole surface of a tree disk. Our computational method involves 10 optical

26 density profiles measured along 10 equally spaced radii drawn from the bark toward the growth axis,
27 and 10 to 20 master rings, that can be easily identified on the whole disk. Growth bands visible on less
28 than 5 radii were discarded. Our method is similar to the cross-dating method used by
29 dendrochronologists, except that it is applied here to a single tree disk. Our samples consist of three
30 disks of *Agathis lanceolata*, one disk of *A. ovata*, and one disk of *Araucaria columnaris*. Multiple
31 regressions have been computed between composite profiles and climatic variables i.e. monthly and
32 yearly temperatures and rainfall amounts. The best correlation is found between the width of the ring
33 growing between July (n-1) and June (n) with the rainfalls of June (n), June (n-1) and June (n-2).
34 Monthly rainfalls allow to explain between 20% to 50% of the ring thickness variance, a result similar
35 to that obtained with other studies on *Agathis* of New Zealand. No temperature parameter appears in
36 the most stable regressions. 30 measurements of tree ring cellulose $\delta^{18}\text{O}$ have been conducted on one
37 single disk selected for the strong climate-ring width correlation. While earlier studies have used $\delta^{18}\text{O}$
38 measurements to identify seasonal cycles in tropical woods and date the rings, our data suggest that
39 the direct use of $\delta^{18}\text{O}$ is misleading due to false rings that do not correspond to a complete growth
40 year. When these false rings are identified from the disk analysis and discarded, a fair visual
41 correlation with the total rainfall during the growth season is obtained. This requires information that
42 cannot be found in single growth band thickness profiles, for example as obtained by coring. Thus,
43 Araucariaceae of New Caledonia may present a valuable potential for dendroclimatology. However,
44 reconstructing a chronology of this region will require more extensive sampling and possibly an
45 account of additional species.

46

47 *Keywords* : dendrochronology; kauri; ENSO; $\delta^{18}\text{O}$; rainfall; New Caledonia

48 **1. Introduction**

49

50 New Caledonia is an island group in the SW Pacific (figure 1) that experience currently El
51 Niño-Southern Oscillation (ENSO) climatic events. During standard conditions, the surface
52 waters of the tropical Pacific ocean are warm (28°C-29°C) in the West and cold (22°-23°C) in
53 the East. The so-called warm water pool is related to increased evaporation and precipitation.
54 During El Niño events, this warm pool is displaced toward the East on the whole equatorial
55 band and the Western Pacific experiences dryer than usual conditions. During the opposite La
56 Niña situation, the warm pool and the associated heavy precipitation zone migrate farther to
57 the West (Philander, 1990). Since ENSO phenomena are dominated by time periods spanning
58 from 3 to 9 yrs, high resolution proxies are required for their study (Rodbell et al., 1999).
59 Continental sedimentary records in New Caledonia provided a 10-100 yrs time resolution
60 (Stevenson et al., 2001; Wirmann et al., 2006). High resolution paleoclimatic studies around
61 New Caledonia mainly rely on coral sampled near the Phare Amedee islet, located 20 km
62 seaward of Noumea, slightly landward of the barrier reef. Quinn et al. (1998) provided $\delta^{18}\text{O}$
63 records in *Porites lutea* since 1657 A.D. which they use to reconstruct past ocean water
64 temperatures. They show also that ocean temperatures measured during the 20th century are
65 fairly well correlated to ENSO. Watanabe et al. (2003)) and Ourbak et al. (2006), working on
66 shorter time series, showed that $\delta^{18}\text{O}$ in *Diploastrea* corals and that Sr/Ca and Mg/Ca in
67 *Porites* corals were temperature-dependent and thus could potentially provide pluricentennial
68 high resolution ocean temperature reconstructions. However, the main island of New
69 Caledonia is a large landmass of nearly 170.000 km² including a continuous central mountain
70 range of an average 1000 m altitude. Its climate should therefore not only be controlled by the
71 ocean.

72 In the temperate climatic zone, and where one climate parameter is a limiting factor
73 for growth, tree rings are widely used to build annually resolved climate reconstructions (e.g.
74 Schweingruber, 1996). In addition, there is growing evidence that tropical trees may also
75 present growth bands related to climatic parameters (Ogden, 1978; D tienne, 1989; Jacoby
76 and D'Arrigo, 1990; Worbes, 1995; Bullock, 1997). It has been demonstrated that during a
77 long dry season the growth of tropical trees stops and that this induces the formation of annual
78 rings in Indonesia (Berlage, 1931), Thailand (Buckley et al., 1995) and in Costa Rica (Enquist
79 and Leffler, 2001). An extensive bibliography of tree ring research in the tropics can be found
80 in Worbes (2002). When annual rings cannot be visually identified, high resolution stable
81 isotopic measurements of wood cellulose may provide a new dating method using the
82 seasonal cycles of cellulose $\delta^{18}\text{O}$ produced in response to the seasonal cycles of tropical
83 precipitation $\delta^{18}\text{O}$ (Evans and Schrag, 2004; Poussard et al., 2004; Poussard and Schrag,
84 2005). In the North Island of New Zealand, 1000 km south of New Caledonia, chronologies
85 of *Agathis australis*, a long-lived rainforest tree, have been established by Buckley et al.
86 (2000).

87 Araucariaceae of New Caledonia include 5 species of *Agathis* and 8 species of
88 *Araucaria*, all endemic, representing 45 % of the species of the family globally (Manaut  et
89 al., 2003). Some of these species are growing on poor ultramafic-derived soils, in particular,
90 *Agathis lanceolata*, which is present as an emergent tree in the rainforest of the south of the
91 main island. Owing to its use as construction material during the 19th century *A. lanceolata*
92 almost disappeared from New Caledonian forests and as a result, it presently benefits from an
93 integral protection. *A. ovata*, another long-living tree endemic to New Caledonia, grows also
94 on ultramafic-derived soils, generally just below mountain passes. Individuals having a trunk
95 circumference of more than 2 m are common. Cherrier and Nasi (1992) have repeated
96 circumference measurements on 146 individuals of *A. ovata* and *A. lanceolata* over a 10 years

97 interval. They deduced a circumference growth of 0.2 to 0.5 cm/yr for *A. lanceolata* and 0.1
98 to 0.5 cm/yr for *A. ovata*. The maximum growth was obtained for samples having a diameter
99 between 60 and 150 cm while some small diameter individuals had almost zero growth.
100 Moreover, it is known that *Agathis* growing in ornamental plantations have larger growth
101 rates than in natural forests, since they are generally planted at a comfortable distance from
102 each other, and they benefit from a soil worked down to near 1 m depth and generally
103 enriched with fertilizer (Whitmore, 1980). The demography of *A. ovata* has also been studied
104 by Enright et al. (2003), who concluded that individuals having a 30 cm diameter at breast
105 height (dbh) could be as old as 700 yrs, and that a dbh of 100 cm could correspond to an age
106 of 1500 yrs. However, their samples consisted mainly of individuals of less than 5 cm dbh.
107 This could explain why the growth rate reported by Enright et al. is less than half the
108 minimum growth rate found by Cherrier and Nasi.

109 During the seventies, the New Caledonian Center of Tropical Trees Studies collected
110 several samples of *A. lanceolata*, which had been marked yearly for 7 years. Nasi and his
111 team (Nasi, 1982) have shown that these trees were producing generally one growth band per
112 year. Some samples, having a dbh of 50 cm, were estimated to be as old as 350 yrs. As some
113 *Agathis* living in New Caledonia are more than 5 m in diameter, this implies that the potential
114 of availability of climatic records is more than a millennium. However, seasons are less
115 marked in New Caledonia than in New Zealand and no relationship between climatic
116 variables and the thickness of growth bands of trees has been proved there. Moreover, Nasi
117 (1982) has shown that *Agathis* produced anomalous growth bands, that were only present on
118 part of the tree circumference. Such anomalous bands are common on tropical trees (Stahle,
119 1999). They have been attributed by Priya and Bhat (1998) to the occurrence of dry periods
120 during rainy seasons, inducing the formation of latewood, or to rainy events during the dry
121 seasons, that promote transient growth. According to the current practice of

122 dendrochronology, growth bands will be termed either as rings, when they are assumed to
123 correspond to a full growth year, or as false rings, if otherwise. In addition, kauris commonly
124 present off-centered growth axes, especially when they grow in windy areas or on steep
125 slopes. This could hinder correct interpretation of cores, which are usually drilled toward the
126 geometrical axis of the tree.

127 The present paper aims to assess the potential for climatic studies of *Agathis*
128 *lanceolata* including comparison with the related species of *A. ovata*, both of which are
129 endemic to New Caledonia and growing on ultramafic soils. These species are compared with
130 *Araucaria columnaris*, using a sample growing on soil derived from continental rocks. In
131 order to gather bidimensional information on growth bands structure, we use whole disks
132 sawn perpendicularly to the trunk at about 1 m height. We will first describe our samples,
133 then the method used to obtain the mean geometric characteristics of rings from a disk.
134 Following this, we discuss the statistical relationship between these geometric characteristics
135 and the climate of New Caledonia. Finally we present 30 $\delta^{18}\text{O}$ measurements made on one of
136 our samples to provide some further clues on their relationship to climatic variables.

137

138 **2. Material**

139

140 ***2.1. Field Sampling***

141

142 The results presented here arise mainly from 3 disks of *A. lanceolata* collected in
143 December, 1981 from three individuals growing inside the Rivière Bleue Provincial Park, 30
144 km north-east of Noumea at 220 m altitude (figure 1). These trees were growing on ultramafic
145 parent soils, that are low in nitrogen, phosphorus, potassium and calcium, but high in iron,
146 magnesium, nickel, chromium, cobalt and manganese (Jaffré, 1980). However, the ultramafic

147 rocks (peridotites) in this area contain several diorite inclusions. During alteration, diorite
148 may provide locally additional nutrients to soils. The sampling area is located only a few
149 meters above a swampy zone, connected to the Yaté artificial lake. Since its construction in
150 1950, the lake flooded the area upstream from the Yaté dam. Five *A. lanceolata* of this area
151 have been marked yearly between 1974 and 1981, at the beginning of each cold season, by
152 opening a 5 cm × 1 cm window across the bark to the cambium. The growth was locally
153 affected by the wounding because of the development of cicatricial tissues but as the
154 wounding is very small compared to the diameter of the trees, this did not impact the overall
155 tree growth rate. Following this, these 5 trees were sawn to provide disks for analysis. As
156 each individual presented generally one growth band between two marks, Nasi (1982) has
157 interpreted these growth bands as annual tree rings. Of these five disks, only three (L1, L2,
158 and L3) are now available. The samples L1, L2, and L3, have circumferences of 155 cm, 153
159 cm, and 165 cm, respectively. From detailed ring counting, Nasi (1982) estimated the ages of
160 L1, L2 and L3 to be 29, 215, and 350 yr, respectively. L1 was an isolated tree, while L2 and
161 L3 were located inside the forest. This and a possible difference in soil composition could
162 explain the higher growth rate of L1. It should be noted that in the upper Rivière Bleue zone,
163 several *A. lanceolata* escaped commercial exploitation during the 19th and 20th centuries and
164 are now more than 5 m in diameter.

165 In order to compare the growth of different species, our study includes a sample of *A.*
166 *ovata* (O1) of dbh 100 cm, growing at 440 m altitude on peridotites, just below the Col du
167 Cintre (figure 1). Since this tree, in contrast to the *Agathis lanceolata* individuals, was
168 growing in a well drained area, perhaps it is more sensitive to drought. Unfortunately, it was
169 partly rotten so that only the external 15 cm could be interpreted. Based on extrapolation of
170 the 150 rings counted within these 15 cm, the whole individual was assumed to contain 400 to
171 500 rings.

172 We included in our study an individual of *Araucaria columnaris* (C1) growing at
173 Noumea (figure 1) on soils derived from a parent rock consisting of alternating silt and clay
174 layers and thus richer in nutrients than ultramafic-derived soils. Our disk was 45 cm in
175 diameter and included about 50 rings.

176 Our limited sampling was insufficient to allow the reconstruction of a chronology
177 from New Caledonian Araucariaceae. Nevertheless, this preliminary study aims to assess the
178 sensitivity to climate of ring thicknesses and the variability of this sensitivity.

179

180

181 ***2.2. Climatic data***

182

183 New Caledonia is situated at the southern limit of the tropical zone and thus benefits
184 from a semi-tropical climate (figure 2). It is exposed to trade winds blowing from the
185 southeast 300 d/yr. Thus, southern New Caledonia, including Noumea, receives a lot of rain.
186 The climate is characterized by a dry season from September to November, followed by rainy
187 and hot season extending from December to March. The climate then cools progressively
188 until June, when the cold season sets in. The optimal growth period of New Caledonian trees
189 spans therefore from December to June. During the hot season, tropical depressions form
190 north of New Caledonia and induce rainy events during their southeastward trajectory. Winter
191 depressions originate from the Coral Sea, situated between New Caledonia and Australia.
192 They consist of cold fronts propagating westward to New Caledonia and are known as "coups
193 d'ouest". Temperature and rainfall data have been recorded in Noumea since 1862. However,
194 several data are missing up to 1899. The mean total annual rainfall is 1100 mm, but large
195 variability results from droughts during El Niño events, and from rainy periods during La
196 Niña events (Morliere and Rebert, 1986) so that extreme rainfall amounts are 500 mm and

197 2000 mm. Nicet and Delcroix (2000) and Manton et al. (2001) have shown in addition that
198 climatic data averaged over the whole New Caledonia were fairly well correlated with SOI,
199 but that this correlation was poor for some individual stations and some time periods. For
200 example, a severe drought was recorded in 1969 in the absence of a El Niño phase, and 1967
201 was very wet during a weak La Niña phase. The mean maximum monthly temperature is
202 32°C in Noumea during the month of January, while the minimum one is 17°C during July,
203 with a low mean daily amplitude of 6°C. The climatic records obtained from Noumea were
204 used in our study, as they are the oldest and the most complete records. However, shorter
205 records spanning a few years to a few decades are also available from various places of south
206 New Caledonia. They show that rainfall increases with altitude and from North to South of
207 the landmass with a monthly distribution similar to that of Noumea (Jaffré, 1980). For
208 example, the station of Montagne des Sources located a few km from our sampling site of
209 *Agathis lanceolata* (L1 to L3) and at a 780 m altitude recorded mean monthly maximal and
210 minimal temperatures of 25°C and 12°C, respectively, and a mean rainfall of 3000 mm.

211 The Southern Oscillation Index (SOI) is widely used to measure the strength of ENSO
212 events (Philander, 1990). This index is calculated from the pressure difference between Tahiti
213 in French Polynesia and Darwin in Australia. It is available for download at
214 <http://ccsm.ucar.edu/cas/catalog/climind/soi.html>. As the SOI is considered as a climatic
215 index in the south Pacific, it will be included in our climatic dataset.

216

217

218 **2. Analysis of growth band distribution**

219

220 *2.1. Determination of mean ring thickness*

221

222 Our 3 disks of *Agathis lanceolata* present off-centered structures with extreme radii of
223 22 and 26 cm, 21 and 24 cm, and 16 cm and 31 cm, for L1, L2, and L3, respectively. The
224 growth bands consist of pale-colored thin walled tracheid (i.e. cells of the xylem) that are
225 limited by dark-colored thick-walled tracheids (figure 3a). But, in contrast to temperate
226 climate conifers, the limits of growth bands is only a few tracheids wide and eventually is
227 discontinuous (figure 3a). Moreover, several growth bands are difficult to detect on the whole
228 circumference due to the fading of their dark limit (figure 3b), or due to wedging of rings
229 (figure 3c). Thus, the band thickness distribution depends on the radius under consideration.
230 This is demonstrated, for example, on the long radius (figure 4b) and the short radius (figure
231 4d) of our sample L3. Starting from the bark and stopping at the same ring boundary at about
232 5 cm from the growth center, we have counted 256 and 356 growth bands along these two
233 radii.

234 In order to use the information present on the whole disk, we have computed the total
235 integrated ring thickness, starting from a digitized image of the disk. First attempts to detect
236 automatically the band limits were unsuccessful due to the following reasons: (i) the optical
237 density and thickness of a given band change along its circumference, (ii) the non constant
238 number of bands along different radii, (iii) the presence of radial structures having an optical
239 density similar to that of band limits (see figure3). However, for our L1 and C1 samples,
240 growth bands were wide enough to be traced directly on a paper on which automatic detection
241 of their limits was worked out. Due to a mean band thickness below 1 mm, and due to the
242 large number of bands, this method could not be applied for our other samples. Our composite
243 method relies on information from 10 equally spaced radii of a disk and from 15-20 master
244 rings visible along the whole circumference. Master rings are commonly used in
245 dendrochronology for cross-dating several tree samples. Usually, they represent years of
246 growth that can be easily identified from several trees from a given area (Schweingruber,

247 1996). In this study, master rings have been used for cross-dating the 10 radii of a single disk.
248 Master rings were first drawn manually on the digitized disk image using the magnetic pen
249 tool of Adobe Photoshop software and were assigned a thickness that makes them easier to
250 detect. The band limits were then numerically detected within 50 pixels wide strips around the
251 10 radii, using the following iterative method: the sum of the optical densities along a series
252 of directions within less than ten degrees from the previous band limit is computed over the
253 50 pixel wide strip. The next band boundary is defined by the direction of maximum
254 cumulated optical density. This direction is then used as the central direction for computing
255 the next band boundary. The first band boundary is assumed to be perpendicular to the radius.
256 This produces a mean optical density profile where band boundaries appear as maxima and
257 the master rings are absolutely black. The detection of band boundaries involves manual
258 adjustment of some parameters for each radius (e.g. mean optical density, width and optical
259 density range for detection of a band limit). Finally, it yields a band limit detection equivalent
260 to manual measurements.

261 The last step consists of integrating the information of the 10 individual radii to
262 compute a mean ring thickness profile. A simple average of the 10 individual profiles will
263 result in a poor signal-to-noise ratio on the mean profile since growth bands from the same
264 time period do not correspond on the different profiles, due to the presence of false rings.
265 Things are not significantly improved if the time scale of each profile is deformed to allow
266 correspondence of the master rings: the different profiles can be averaged only on a narrow
267 zone around each master ring, as long as no incomplete ring is observed. This led us to
268 identify incomplete rings and to introduce a zero thickness band when they are not present on
269 a given profile. Starting from the longest radius, such a zero thickness growth band is inserted
270 in the next profiles at each place where a band disappears. It is assumed that the thinnest
271 bands are the most likely to disappear. Then growth bands present on less than 5 radii are

272 considered as false rings, and the thicknesses of true rings are averaged to produce the mean
273 profile. This arbitrary limit of 5 radii produces a composite profile with the same number of
274 rings as that of the longest radius. This implies that the number of false rings on this radius is
275 equal to the number of rings which cannot be detected on it, although they are considered as
276 true annual rings, since they are present on more than 5 other radii. The threshold of 5 radii
277 complies with the result obtained by Nasi (1982) from annual marking of 12 different trees
278 during seven successive years. Moreover, this value maximizes the correlation with climatic
279 data (see below). However, since it is established on a statistical basis, our composite profile
280 may include some false rings, while some true rings are lacking. Figure 4 represents the ring
281 thicknesses obtained for L3 along the long radius, the short radius, and the composite profile.
282 They are compared with climatic data recorded in Noumea and with the SOI. In the next
283 sections, we apply signal analysis methods to assess the climatic information included in these
284 composite profiles.

285

286 *2.2. Spectral density analysis*

287

288 Some of our profiles seem to present periodicities, which led us to a preliminary
289 frequency analysis. Since spectral analysis is not the main topic of the paper, a simple and
290 robust method is adopted here. As the Fourier transform of the signal is known to produce
291 noisy spectra, the Fourier transform of the autocorrelation function is used here instead (Press
292 et al., 1992). Taking the autocorrelation enhances periodic components of the signal.
293 Moreover, the larger lag components of the autocorrelation function, which are those who
294 introduce noise in the spectrum, are discarded with windowing techniques. This method is
295 easy to implement, robust (Oppenheim and Shafer, 1974) and may be applied for various
296 length data such as our three ring thickness profiles. The composite profile of L3 presents

297 only one noticeable period at 22 yrs, while the short radius does not present any clear
298 periodicity and the long one exhibits only one peak at 6.6 yrs. Our sample L2 did not produce
299 any marked periodicity, while O1 presents marked periods at 28, 17 and 8 yrs. For the
300 climatic variables, rainfall data present a smooth peak at 20 yr and a large spectral content for
301 periods longer than 4 yrs without any clear additional peak, while temperature presents two
302 marked peaks at 21 and 2.3 yrs. These results confirm the visual impression that our samples
303 present marked periodicities. The 20-22 yrs period is present in L3, in the temperature and in
304 rainfall data. This could indicate that a common process having a near 20 yr period is present
305 in our observations and that it has been undersampled in O1, probably because several annual
306 rings are absent on this profile. This period is also present in the Interdecadal Pacific
307 Oscillation which has been shown to modulate ENSO (Folland et al., 1999; Salinger et al.,
308 2001). As a whole, the tree growth spectra present little power near the frequencies commonly
309 associated to ENSO, while temperature and rain present power near 2.3 yr and 4 yr, i.e. close
310 to 3.2 yr, which Quinn et al. 1998 found the most reliable period in SOI. This could result
311 from the large noise introduced up to a few years period by the imperfect false ring
312 identification. Besides, data sampled at near a one year time interval such as tree rings are not
313 perfect for the definition a signal at a few years period. The spectral approach deserves further
314 exploration using more sophisticated methods when a larger sample set becomes available. It
315 could help to select the individuals presenting the best correlation with climate.

316

317 *2.3. Correlation analysis*

318

319 Figure 5 represents the ring thicknesses recorded in the profiles of all our samples and
320 the climatic variables of figure 4. The relationship between tree ring thickness and climatic
321 variables is not obvious. This leads us to a statistical analysis of the correlation between tree

322 rings and climate. We used monthly temperatures and rainfalls as well as cumulated rainfall
323 on various time periods, i.e. during the wet season, the dry season and the growth season, that
324 is assumed to extend from July until June of the following year. Annual temperatures and
325 rainfall as well as the SOI have also been considered.

326 The method used is multiple regression of the Statistical Analysis Software (SAS
327 Institute, 2004). At each step, this method extracts the variable corresponding to the largest
328 explained variance, using partial least squares. This variable is added to the regression if it
329 corresponds to a Pvalue of the Fisher test of less than 5%. When a variable is added to the
330 regression, all the previous variables are considered again, and those corresponding to a
331 Pvalue less than 5% are ruled out. This method is well suited for highly correlated variables,
332 such as our climatic data (Radhakrishna and Rao, 1967; Wang and Chow, 1994). In order to
333 include non linear combinations of climatic variables, tests were also performed with their
334 logarithms, since adding logarithms results in the logarithm of the product of the variables,
335 but these tests did not allow the extraction of any significant variable.

336 The correlation results are summarized in table 1. Monthly rainfalls are denoted by P,
337 followed by the name of the month and the number of the year. so that PJune(n) is the rainfall
338 of the month of June of the growth season. Correlations have also been computed for different
339 radii numbers on which a growth band should be present to be considered as a true ring. This
340 resulted in a broad maximum for 5 radii. Therefore this value has be adopted to build the
341 composite profiles. The first observation is that temperature does not appear in this table. This
342 does not mean that temperature does not influence growth, since rainfall and temperature are
343 correlated. In fact, generally negative yet significant correlations appear with monthly
344 temperatures if rainfalls are discarded from our analysis. Such correlations have also been
345 found by Buckley et al. (2000) for kauris of Northern New Zealand. However, these
346 correlations vary largely between our individuals, even if they belong to the same species.

347 The second observation is that only low total or partial explained variance can be
348 obtained. Thus, our data have also been run with the DENDROCLIM software, which is
349 devoted to cross correlation analysis of tree rings and has been benchmarked by Biondi and
350 Waikul (2004). When using our sample L3, for which the best correlations with climate have
351 been found by SAS (see table 1), the only significant correlations given by DENDROCLIM
352 are those with the rainfall of June of the year preceding growth, and with the rainfall of June
353 of the year before, with correlations of 0.37 and 0.24. Since the correlation coefficients are the
354 square root of the explained variances, the corresponding explained variances are 0.14 and
355 0.06, respectively, which are exactly those found by SAS. The reduced number of significant
356 climatic variables found by DENDROCLIM may result from the computation of the error in
357 the correlation, based on the bootstrap method, while SAS uses the results of least squares.
358 Our correlation coefficients are similar to those found by Buckley et al. (2000) with the kauris
359 of New Zealand. We prefer however, to further use the explained variances (R^2) of table 1
360 since they are additive and provide the total explained variance. Table 1 also shows that the
361 R^2 coefficients vary according to the individual sampled, even for the 3 *A. lanceolata*
362 individuals, that were located within an area of 100 m radius. Our samples L2 and L3,
363 although presenting similar growth rates, do not exhibit the same correlations with climate.
364 Based on our correlation analysis, the sample L3, only, will be suitable for building future
365 chronologies of New Caledonia.

366 However, it is noteworthy to notice that all our samples present a statistically
367 significant correlation with the rainfall of the month of June of the growing season, of the
368 previous season, or with that of the year before. We have verified that this correlation relied
369 only on external rings. This is an indication that no systematic over-or-undersampling is
370 introduced in our ring counting process. The correlation with PJune (n-1) and PJune(n-2) may
371 be due to the accumulation of nutrients in the root of the tree, which are used during the

372 coming growing seasons extending from July to June of the following years. Accumulation in
373 the root system of carbohydrates which are further used during a growth season is common
374 for trees (see for example Jacoby and D'Arrigo, 1990). The correlation with PJune(n-1) and
375 PJune(n-2) observed for our sample L3 may be an indication either that for a poor soil and a
376 very thin organic cover, accumulation of nutrients inside the root system may be needed for
377 more than one year before growth, or that one true ring has been misinterpreted as a false ring
378 in the external part of this sample so that all inner rings are shifted one year in the past. On the
379 other hand, higher rainfall during June(n) may extend the duration of the growth season,
380 which could explain the positive correlation with PJune(n). The presence of Pjuly in two of
381 the regressions could reinforce these hypotheses.

382 For our sample L3, presenting the best correlations with climate, it appears that these
383 correlations are only obtained with the composite profile while the individual profiles present
384 much lower correlations. As a consequence, our results can not be applied to data obtained by
385 coring. As the individual radii of L3, however, present correlation with climate similar to
386 those obtained with the single profile of O1, we suspect that a whole disk of *A. ovata* could
387 provide a valuable climatic proxy.

388

389 **3. $\delta^{18}\text{O}$ profiling**

390

391 Isotopic composition of the tree cellulose is known to provide information on the
392 annual rainfall of temperate climates (Raffali-Delerce et al., 2004). Poussard et al. (2004)
393 have recently shown that $\delta^{13}\text{C}$ and $\delta^{18}\text{O}$ measured in cellulose of some tropical species were
394 also linked to climate. Recall that $\delta^{18}\text{O}$ measurements are defined as the relative difference
395 between the $^{18}\text{O}/^{16}\text{O}$ ratio of the sample and that of the SMOW standard. We have measured
396 $\delta^{18}\text{O}$ of the α -cellulose of the 30 external growth bands of the longest radius of L3. One of the

397 widest of these 30 bands has been divided into four parts to check the variability of the
398 oxygen isotopic composition inside a single band. A strip 2 cm wide and 0.5 cm thick has
399 been sawn along this long radius and each ring cut out, then grinded and mixed. The α -
400 cellulose from two samples of 0.25 mg of each of these bands has been extracted following
401 the method discussed in Green (1963) and Leavitt and Danzer (1993) and analyzed for $\delta^{18}\text{O}$.
402 The precision of the measurements has been estimated to 0.25‰, which is the standard
403 deviation of repeated measurements of Raffali-Delerce et al. (2004). Thus, values from the
404 two samples were averaged if these values differed by less than 0.25‰, and if not, they were
405 discarded. Given the insufficient length of our sampling, the SAS regression procedure could
406 not be used, since it involves monthly and annual rainfall and temperature of the growth year
407 and of the two precedent years, i.e. 78 climatic data. Thus, its is likely that a reasonable fit of
408 our 30 $\delta^{18}\text{O}$ measurements could have been found, even if they were perfectly random.

409 Our measurements have been, therefore, directly compared with the total rainfall of
410 the growing season (figure 6), which has been shown to be proportional to $\delta^{18}\text{O}$ in both
411 temperate (Raffali et al., 2004) and tropical climates (Poussard et al., 2004; Poussard and
412 Schrag 2005). The scale $\delta^{18}\text{O}$ scale in figure 6 has been reversed to emphasize the
413 anticorrelation with rainfall. If each ring of our radius is assumed to correspond to a growth
414 year, the correlation between $\delta^{18}\text{O}$ and the annual rainfall is weak (figure 6), except for the
415 last 7 growth bands, for which the annual marks of Nasi (1982) demonstrate that one growth
416 band was produced per year. This led us to use the composite profile of L3 obtained in the
417 previous section to identify the false rings and possible missing rings within our sampled strip
418 of L3. Several false rings, including 2 sets of successive 3 false rings were identified within
419 these 30 sampled bands. They are marked in bold on figure 6. It is also notable that the two
420 samples presenting larger than 0.25‰ discrepancy between their two $\delta^{18}\text{O}$ measurements also
421 corresponded to false rings (dotted bold segments in figure 6). When measurements

422 corresponding to false rings are discarded, the $\delta^{18}\text{O}$ profile is visually similar to that of the
423 annual rainfall. We have verified that this profile was only slightly changed if measurements
424 from the false rings were averaged with that of the following or of the previous true ring.
425 However, the visual relationship between $\delta^{18}\text{O}$ and rainfall only produces of a low correlation
426 of -0.18. Careful examination of both curves show that, although similar in shape, they
427 usually present an offset of 1 yr , and that the correlation seems to be inversed between 1965
428 and 1968. This suggests that either small random time offsets persist in our composite profile
429 or that the $\delta^{18}\text{O}$ signature of a ring does not depend only on the rainfall during its growth year,
430 a result also indicated by the correlation of ring thickness with the years preceding the growth
431 year. Thus, our results could be improved by a better identification of the rings and a better
432 knowledge of the conditions capable of inducing the formation of multiple growth bands
433 during a single growth year.

434 Moreover, $\delta^{18}\text{O}$ may be not only correlated with annual rainfall but also with the
435 geographical origin of rainy events. Further discussion on the origin of $\delta^{18}\text{O}$ signature of tree
436 rings would require $\delta^{18}\text{O}$ data for rain, surface waters and groundwaters of New Caledonia,
437 which are for the moment not available. On the other hand, the multi-sampling of the widest
438 growth band of our strip did not indicate any relation with climatic details inside its growth
439 year, in contrast with the results of Poussard and Schrag (2005). It is concluded from our
440 results that more extensive $\delta^{18}\text{O}$ sampling is needed in New Caledonia.

441

442 **4. Summary and conclusion**

443

444 Growth bands can easily be observed in New Caledonia Araucariaceae. However it is
445 known that kauris may produce several bands during a single year (Boswijk et al., 2006).
446 These bands are generally present only on a part of the trunk circumference and should not be

447 considered for reconstructing a chronology. Similarly, a true annual ring may also be present
448 only on a part of the circumference. Moreover, as the growth axis of these trees is generally
449 off-centered, ring profiles obtained by coring without a previous knowledge of the growth
450 axis may be difficult to interpret as opposed to full disks sawn perpendicularly to the trunk.

451 Our 5 tree samples were gathered in the South New Caledonia, a region subjected to
452 ENSO events and characterized by poor ultramafic-derived soils. Three of them are older than
453 200 yrs. We have computed composite ring thickness profiles, integrating information from a
454 full disk, starting from automatic identification of growth band limits along 10 equally spaced
455 radii and manual drawing of 10 to 20 master rings on the whole circumference of the disk. We
456 assumed that bands present on less than half a complete circumference should be discarded.
457 This criterion complies with observations of bands produced between annual marks during the
458 seven year experiment of Nasi (1982) and also produces the best correlation between
459 composite ring profiles and climate. However, as this criterion is only valid on a statistical
460 basis, it may lead to some wrong identifications of true rings and false rings. Moreover,
461 information regarding the maximum optical density of latewood is not retained in the
462 composite profile.

463 Our study includes 10 individual profiles from 4 disks plus one radius from the fifth
464 disk, giving a total of 41 profiles, which is much lower than those used by Buckley et al.
465 (2000) to build their chronology of Northern New Zealand on kauris. Consequently, the
466 present study should only be considered as an assessment of the potential of New Caledonian
467 Araucariaceae for future dendrochronology studies.

468 Climatic data of New Caledonia only explain a low part of the variance of our ring
469 profiles. Significant (i.e. Pvalue <5% in Fisher test) correlation is found with monthly
470 temperatures but the annual rainfall only appears after the multiple regression process. This
471 does not mean that the growth of our species does not depend on temperature, but that the

472 regression with the annual rainfall is more stable. This implies that information related to
473 rainfall rather than to temperature is likely to be obtained from tree ring studies in New
474 Caledonia. For our samples, interannual variability of monthly rainfall amounts allows
475 explanation of between 20% and 50% of the ring thickness variability, and less than 37% if
476 the sample is older than 100 yrs. It should be emphasized that the correlation coefficients
477 (square root of explained variance) with monthly rainfalls are similar to those obtained by
478 Buckley et al. (2000) for kauris of New Zealand.

479 A correlation with the rainfall of June (n) (i.e. following growth) or June (n-1)
480 (preceding growth) arises in almost all our samples, whatever the species, the location,
481 altitude or the soil of the sampling site. This month marks the onset of the cool season lasting
482 until September, followed by the dry season until December. Therefore, it may be considered
483 that the month of June marks the beginning of the slow growth season and that a high rainfall
484 during June may increase the duration of this growth or allow accumulation of nutrients for
485 later use.

486 30 measurements of tree ring cellulose $\delta^{18}\text{O}$ have been conducted on one single disk
487 selected for its better climate-ring width correlation. While earlier studies have used $\delta^{18}\text{O}$
488 measurements to identify seasonal cycles in tropical woods and date the rings, our data
489 suggest that the direct use of $\delta^{18}\text{O}$ is misleading due to false rings that do not correspond to a
490 complete growth year. When these false rings are identified from the disk analysis and
491 discarded, data from the external part of our sample L3 present a general pattern
492 anticorrelated with that of annual rainfall during the growth season (July(n-1) to June(n)).
493 However, a slight random offset of 1 yr between $\delta^{18}\text{O}$ and annual rainfall and a 4 yr period
494 where the correlation is reversed yielded a correlation of only -0.18. We note that false rings
495 could not have been discarded without our composite profile, relying on the information of
496 the whole disk. Additional $\delta^{18}\text{O}$ data on Araucariaceae of New Caledonia are needed to assess

497 more precisely their relationship with the climate. Poussard et al. (2004) and Poussard and
498 Schrag (2005) have shown that dense sampling inside rings allows detection of the variation
499 of the climate inside a single year. This deserves a systematic study in New Caledonia to
500 assess the ability of this method to detect false rings.

501 Our results rely on a reduced sampling. They have to be confirmed by more data on
502 tree rings in New Caledonia. Moreover due to the low correlation found with climate, a large
503 number of samples and/or careful sample selection will be required to build a chronology. As
504 individuals of *A. lanceolata* larger than a few meters in diameter are known in New
505 Caledonia, accumulating tree ring data may lead to a chronology on a time period of 500-
506 1000 yr.

507

508 **Aknowldgments**

509

510 Isotope analyses have been partly funded by the French CNRS/INSU ECLIPSE
511 program. The staff of the Rivière Bleue Reserve and Parc Forestier of Noumea are warmly
512 acknowledged for their help in collecting samples, and likely Meteo France for providing
513 access to their climatic database. Discussion with J. Tassin (CIRAD Forest), J.P. Ricci (DRN
514 Noumea) as well as V.D. Dang were fruitful at the onset of this project. This work benefited
515 from the help from Jocelyne Bonneau for ring counting and samplingn, from Gregory Lasne
516 for photography and from Alain Courtot for woodwork. Comments from one associate editor
517 and from two reviewers helped to improve the manuscript.

518

519 **References**

520

521 Atlas climatique de la Nouvelle Calédonie, 1995, Météo-France, Noumea, 103p.

522 Berlage, H.P., 1931. Over het verband tusschen de dikte der jaarringen van djatiboomen
523 (Tectona grandis L. f.) en den regenval op Java. Tectona, 24, 939-953.

524 Biondi, F., Waikul, K., 2004. DENDROCLIM2002: A C++ program for statistical calibration
525 of climate signal in tree-ring chronologies. Comp. and Geosci., 30, 303-311.

526 Boswijk, G., Fowler, A., Lorrey, A., Palmer, J., Ogden, J., 2006. Extension of the New
527 Zealand kauri (*Agathis australis*) chronology to 1724 AC. The Holocene, 16, 188-189.

528 Buckley, B.M., Barbetti, M., Watanasak, M., D'Arrigo, R., Boonchirdchoo, S., Sarutanon, S.,
529 1995. Dendrochronological investigation in Thailand. Int. Assoc. Wood Anatomists J., 16,
530 393-409.

531 Buckley, B., Ogden, J., Palmer, J., Fowler, A., Salinger, J., 2000. Dendroclimatic
532 interpretation of tree-rings in *Agathis australis* (kauri). 1. Climate correlation functions
533 and master chronology. J. R. Soc. New Zealand, 20, 263-275.

534 Bullock, S.H., 1997. Effects of seasonal rainfall on radial growth in two tropical tree species.
535 Int. J. of Biometeorology, 41, 13-16.

536 Cherrier, J.F., and Nasi, R. 1992. Placettes de suivi de croissance en forêt naturelle de
537 Nouvelle Calédonie. Report CIRAD-CTFR, Noumea.

538 Détienne, P., 1989. Appearance and periodicity of growth rings in some tropical woods. Int.
539 Assoc. Wood Anatomists Bull., 10, 123-132.

540 Enquist, J.B., Leffler, A.J., 2001. Long-term tree ring chronologies from sympatric tropical
541 dry-forest trees: individual response to climatic variations. J. Tropic. Ecol., 17, 41-60.

542 Enright, N.J., Miller, B.P., Perry, G.L.W., 2003. Demography of the long-lived conifer
543 *Agathis ovata* in maquis and rainforest, New Caledonia. J. Veg. Sci., 14, 625-636.

544 Evans, M.N., Schrag, D., 2004. A stable isotope-based approach to tropical
545 dendroclimatology. Geochim. Cosmochim. Acta, 68, 3295-3305.

546 Folland, C.K., Parker, D.E., Colman, A.W., Washington, R., 1999. Large scale modes of
547 ocean surface temperature since the late nineteenth century. In: Beyond El Niño: decadal
548 and interdecadal variability, Navarra, A. (Ed.), Springer, Berlin, pp. 73-102.

549 Green, J.W., 1963. Wood cellulose. In: Method of Carbohydrate Chemistry, III, R.L. Whisler
550 (Eds), Academic Press, New York, pp. 9-20.

551 Jacoby, G.C., 1989. Overview of tree-ring analysis in tropical regions. Int. Assoc. Wood
552 Anatomists Bull., 10, 99-108.

553 Jacoby, G.C., D'Arrigo, R., 1990. Teak (*Tectona Gandis L.F.*), a tropical species of large-
554 scale dendroclimatic potential. *Dendrochronologia*, 8, 83-98.

555 Jaffré, T., 1980. Etude écologique du peuplement végétal des sols dérivés des roches
556 ultrabasiqes en Nouvelle Calédonie, Travaux et documents de l'ORSTOM No 124,
557 ORSTOM, Paris.

558 Leavitt, S.W., Danzer, S.R., 1993. Method for batch processing small wood samples to
559 holocellulose for stable carbon isotope analysis. *Ann. Chem.*, 65, 87-89.

560 Manauté, J., Jaffré, T., Veillon, J.M., Kranitz, M.L., 2003. Revue des araucariaceae de
561 Nouvelle Calédonie. IRD/Province Sud of New Caledonia, Noumea, New Caledonia.

562 Manton, M.J., Della-Marta, P.M., Haylock, M.R., Hennesy, K.J., Nicholls, N., Chambers,
563 L.E., Collins, D.A., Daw, G., Finet, A., Gunawan, K., Inape, H., Isobe, T.S., Kestin, T.S.,
564 Lefale, P., Leyu, C.H. Lwin, T., Maitrepierre, N., Ouprasitwong, N., Page, C.M., Pahalad,
565 J., Plummer, N., Salinger, M.J., Suppiah, R., Tran, V.L., Trewin, B., Tibig, I., Yee, D.,
566 2001. Trends in extreme daily rainfall and temperature in Southeast Asia and the South
567 Pacific: 1961-1998. *Int. J. Climatol.*, 21, 269-284.

568 Morliere, A., Rebert, J. P., 1986. Rainfall shortage and El Niño-Southern Oscillation in New
569 Caledonia, Southwestern Pacific. *Mon. Wea. Rev.*, 114, 1131-1137.

570 Nasi R., 1982. Essai pour une meilleure connaissance et une meilleure compréhension des
571 araucariacées dans la végétation calédonienne. Mémoire d'Ingénieur, GERDAT-CTFT,
572 Nogent sur Marne, France.

573 Nicet, B., Delcroix, T., 2000. ENSO-related precipitation changes in New Caledonia,
574 Southwestern tropical Pacific: 1969-98. Mon. Wea. Rev., 128, 3001-3006.

575 Ogden, J., 1978. On the dendrochronological potential of Australian trees. Aust. J. Ecol., 3,
576 339-356.

577 Oppenheim, A.V., Schafer, R.W., 1974. Digital signal processing. Prentice Hall, Englewood
578 Cliffs, N.J., USA.

579 Ourbak, T., Correge, T., Malaize, B., Le Cornec F., Charlier K., Peypoupet, J. P., 2006. A
580 high-resolution investigation of temperature, salinity, and upwelling activity proxies in
581 corals. Geochem. Geophys. Geosyst., 7, Q03013, doi:10.1029/2005GC001064.

582 Philander, S.G.H., 1990. El Niño, La Niña and the Southern Oscillation. Academic Press, San
583 Diego, CA.

584 Poussard, P.F., Evans, M.N., Schrag, D.P., 2004. Resolving seasonality in tropical trees:
585 multi-decade high resolution oxygen and carbon isotope record from Indonesia and
586 Thailand. Earth Planet. Sci. Lett. 218, 301-316.

587 Poussard P.F., Schrag, D.P., 2005. Seasonally stable isotope chronologies from northern
588 Thailand deciduous trees. Earth. Planet. Sci. Lett., 235, 752-765.

589 Press, W.H., Teukolsky, S.A., Vetterling, W.T., Flannery, B.P., 1992. Numerical recipes in
590 Fortran. The Art of Scientific Computing, 2nd ed. Cambridge University Press, New
591 York, NY, USA.

592 Priya, P.B., Bhat, K.M., 1998. False ring formation in teak (*Tectona grandis* L.f.) and the
593 influence of environmental factors. Forest Ecol. Manag., 108, 215-222.

594 Quinn, W.H., Crowley, T.J., Taylor F.W., Hénin, C., Joannot P., Join, Y., 1998. A multi-
595 century stable isotope record from a New Caledonia Coral : Interannual and decadal sea
596 surface temperature variability in the souhtwest Pacific since 1657 AD.
597 *Paleoceanography*, 13, 412-426.

598 Radhakrishna, C., Rao, J., 1967. *Linear statistical inference and its application*. John Wiley
599 and Sons, New York.

600 Raffalli-Delerce G., Masson-Delmotte V., Dupouey J.L., Stievenard M., Breda N., Moisselin
601 J.M. 2004. Reconstruction of summer droughts using tree-ring cellulose isotopes: a
602 calibration study with living oaks from Brittany (western France). *Tellus*, 56-2, 160-174.

603 Rodbell, D. T., Seltzer G. O., Anderson, D. M., Abbott, M. B., Enfield, D. B., Newmann, J.
604 H., 1999. An~15,000-year record of El Niño-driven alluviation in southwestern Ecuador.
605 *Science*, 4401, 516-520.

606 Salinger, M.J., Renwik, J.A., Mullan, A.B., 2001. Interdecadal Pacific Oscillation and South
607 Pacific climate. *Int. J. Climatol.*, 21, 1705-1721.

608 SAS Institute, 2004. *SAS/STAT 9.1 user's guide*, SAS Institute Inc., Cary, NC.

609 Schweingruber, F.H., 1996. *Tree rings and Environment Dendroecology*. Haupt, Vienna.

610 Stahle, D., 1999. Useful strategies for the development of tropical tree-ring chronologies. *Int.*
611 *Assoc. Wood Anatomists J.*, 20, 249-253.

612 Stevenson, J., Dodson, J.R., Prosser, L.P., 2001. A late Quaternary record of environmental
613 change and human impact from New Caledonia. *Paleogeog. Paleoclimatol. Paleoecol.*,
614 168, 97-123.

615 Wang, S.G., Chow, S.C., 1994. *Advanced linear models : theory and applications*. Marcel
616 Dekker, New York, pp. 146-223.

617 Watanabe, T., Gagan, M.K., Corregge, T., Scott-Gagan, H., Cowley, J., Hantoro, W.S., 2003.
618 Oxygen isotope systematic in *Diploastrea-heliopora* : new coral archive of tropical
619 paleoclimate. *Geochim. Cosmochim. Acta*, 67, 1349-1358.

620 Whitmore T.C., 1980. A monograph on *Agathis*. *Plants Systematics and Evolution*, 135, 41-
621 69.

622 Wirrmann, D., Semah, A.M., Chacornac-Rault, M. 2006. Late Holocene paleoenvironment in
623 northern New Caledonia, Southwestern Pacific, from a multiproxy analysis of lake
624 sediments. *Quat. Res.*, 66, 213-232.

625 Worbes, M., 1995. How to measure growth dynamics in tropical trees: a review. *Int. Assoc.*
626 *Wood Anatomists J.*, 16, 337-351.

627 Worbes, M., 2002. One hundred years of tree-ring research in the tropics - a brief history and
628 an outlook to future challenges. *Dendrochronologia* 20, 217-231.

629

630 **Figure captions**

631

632 Figure 1. Location of the sampling area, and of New Caledonia in the southwest Pacific
633 (inlet). Each sampling area is labeled by its sample reference. L1-L3 correspond to the three
634 *A. lanceolata*, O1 to the *A. ovata*, and C1 to the *Araucaria columnaris*. The greyed area
635 figures the extent of the southern ultramafic massif.

636

637 Figure 2. Mean climate of Noumea (1888-2004). The bar chart shows the annual rainfall and
638 the curve shows the mean monthly temperature.

639

640 Figure 3. Ring structure of *A. lanceolata*. a) The limits of growth bands (vertical arrows)
641 consists of a thin and discontinuous series of thick-walled dark-colored tracheids. b) Fading of
642 a ring limit (horizontal arrow) from right to left. This ring limit cannot be detected at the left
643 end of the picture. c) a series of wedging rings (horizontal arrow), where decreasing width
644 rings merge together (from right to left). Radial structures perpendicular to rings with the
645 same optical density as ring limits may be observed on these three pictures.

646

647 Figure 4. Comparison of the climatic data with the different ring thickness profiles from L3.
648 a): Climatic data: annual rainfall during the growth season, i.e. July to June (solid bars), and
649 mean annual temperature (solid line), both recorded in Noumea. The SOI index, averaged on
650 a 1 yr moving window, is represented with a dashed line (arbitrary unit). Growth band
651 thicknesses (arbitrary units) of our L3 sample along the longest radius (b), the composite
652 profile, averaged on the whole disk (c) and the short radius (d).

653

654 Figure 5. Comparison of thickness profiles recorded with our different samples (arbitrary
655 vertical units, vertical scale at the right). The annual temperature and rainfall of figure 1 are
656 also indicated at the top of the figure. Note that O1 corresponds to a single profile while the
657 other samples correspond to synthetic profiles averaged over the whole disk. For L3 and L2,
658 the 100 last years, only are displayed, since for older rings no correlation with climatic data is
659 possible.

660

661 Figure 6. Comparison between $\delta^{18}\text{O}$ measured in L3 with the annual rainfall during a growth
662 year (July of a given year until June of the following year). Top: rainfall; bottom: $\delta^{18}\text{O}$ data.
663 In order to emphasize the anticorrelation with annual rainfall, the $\delta^{18}\text{O}$ axis has been
664 reversed. The black curve, including dotted and thick parts represents raw data. Data from
665 false rings are indicated in bold. False rings where two measurements resulted in a $\delta^{18}\text{O}$
666 discrepancy of more than 0.25‰ (see text) correspond to the dotted segments. In the red
667 curve, false ring data have been discarded. Both $\delta^{18}\text{O}$ curves are identical in the external part
668 of L3, where the annual marks indicate that there are no false rings.

Table 1

[Click here to download Table: table1.doc](#)

Correlation between tree ring thickness and monthly rainfalls			
Variable	Explained variance (R ²)	Cumulated explained variance	Pvalue
ARAUCARIA COLUMNARIS (C1)			
Pjune (n)	0.18	0.18	0.0125
Pjune (n-1)	0.14	0.32	0.0161
Pmay (n)	0.08	0.41	0.036
Papril (n-1)	0.09	0.5	0.0425
AGATHIS LANCEOLATA (L1)			
Pdecember (n-1)	0.216	0.216	0.0192
AGATHIS LANCEOLATA (L2)			
Pjune (n)	0.05	0.05	0.0133
Papril (n-2)	0.05	0.10	0.0147
Pjuly (n-2)	0.06	0.16	0.0167
Pmay (n-2)	0.04	0.20	0.0328
Pjune (n-1)	0.04	0.24	0.0471
Pjuly (n-1)	0.04	0.28	0.0471
AGATHIS LANCEOLATA (L3)			
Pjune (n-1)	0.14	0.14	0.0001
Pjune (n-2)	0.06	0.20	0.0109
Pdecember (n-1)	0.05	0.25	0.0147
N. dry months (n)	0.05	0.30	0.0196
Pjanuary (n-1)	0.04	0.34	0.0337
Pdecember (n-2)	0.03	0.37	0.0347
AGATHIS OVATA (O1)			
Pdecember (n-2)	0.06	0.06	0.0110
Pjuly (n)	0.05	0.11	0.0264
Pjune (n-1)	0.05	0.16	0.0366
Pjune (n)	0.05	0.21	0.0379

Table 1

Figure 1

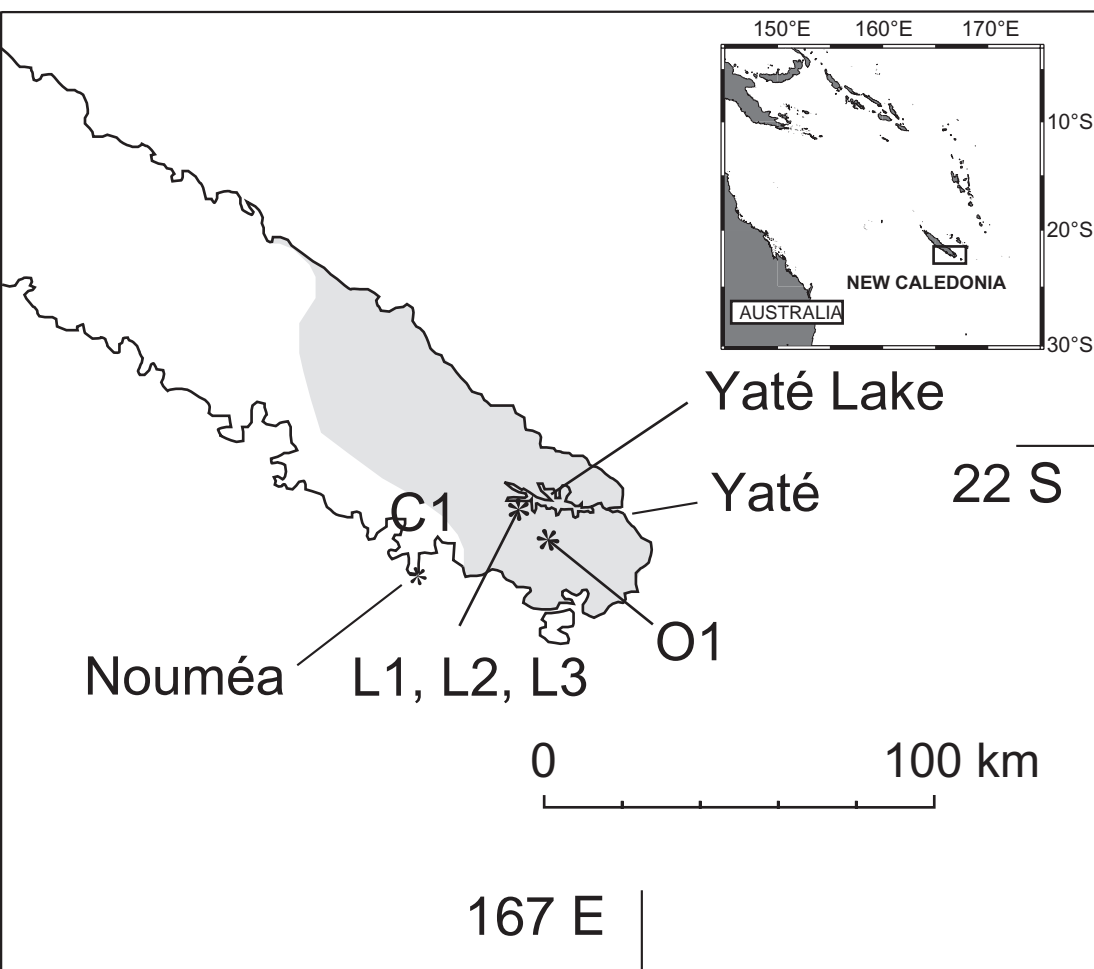


Figure 1 Liebeau et al.

Figure 2

Figure 2 Lieubeau et al.

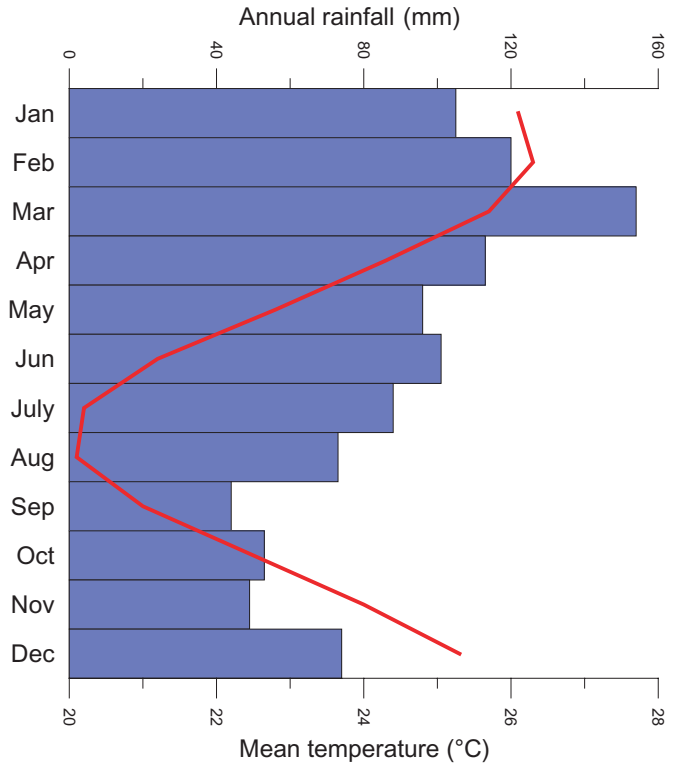


Figure 3

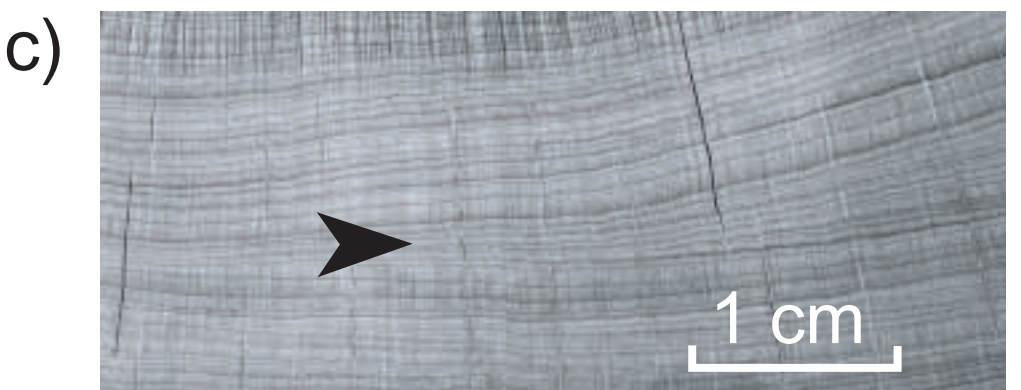
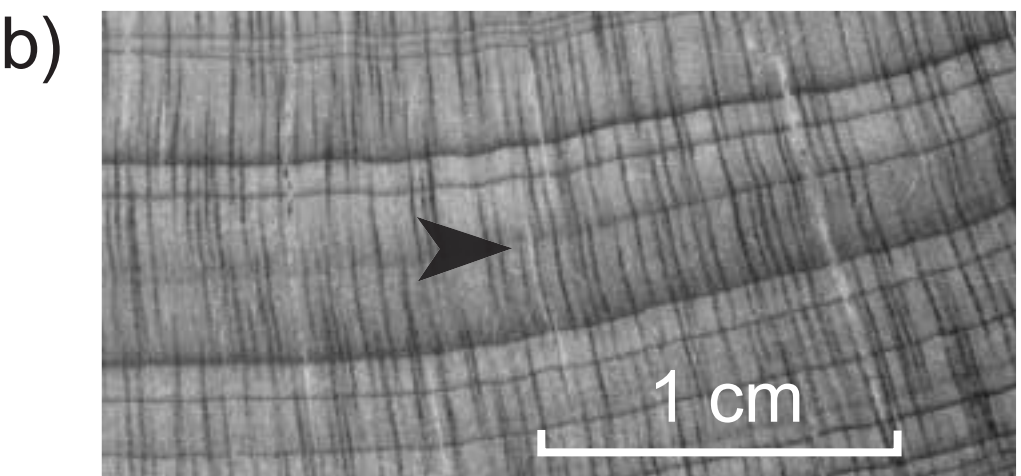
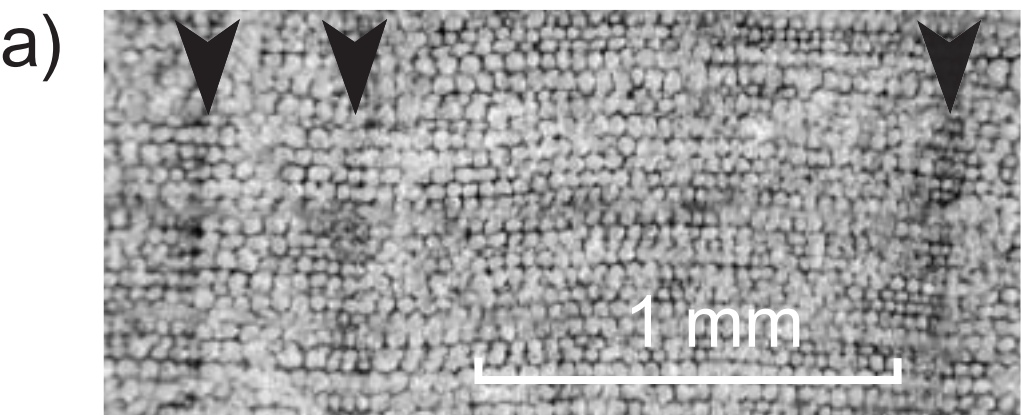


Figure 3 Lieubeau et al.

Figure 4

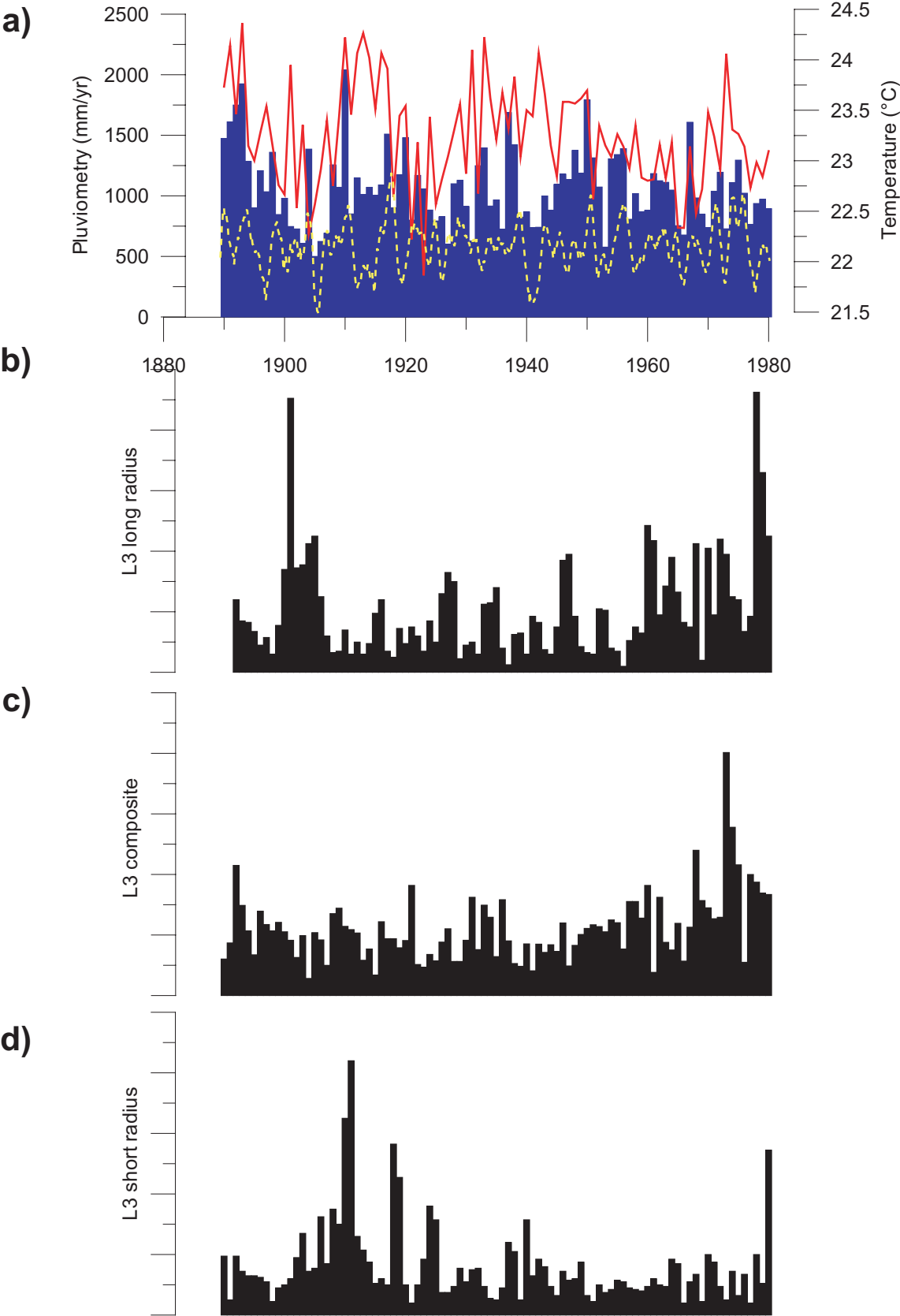


Figure 4 Lieubeau et al.

Figure 5

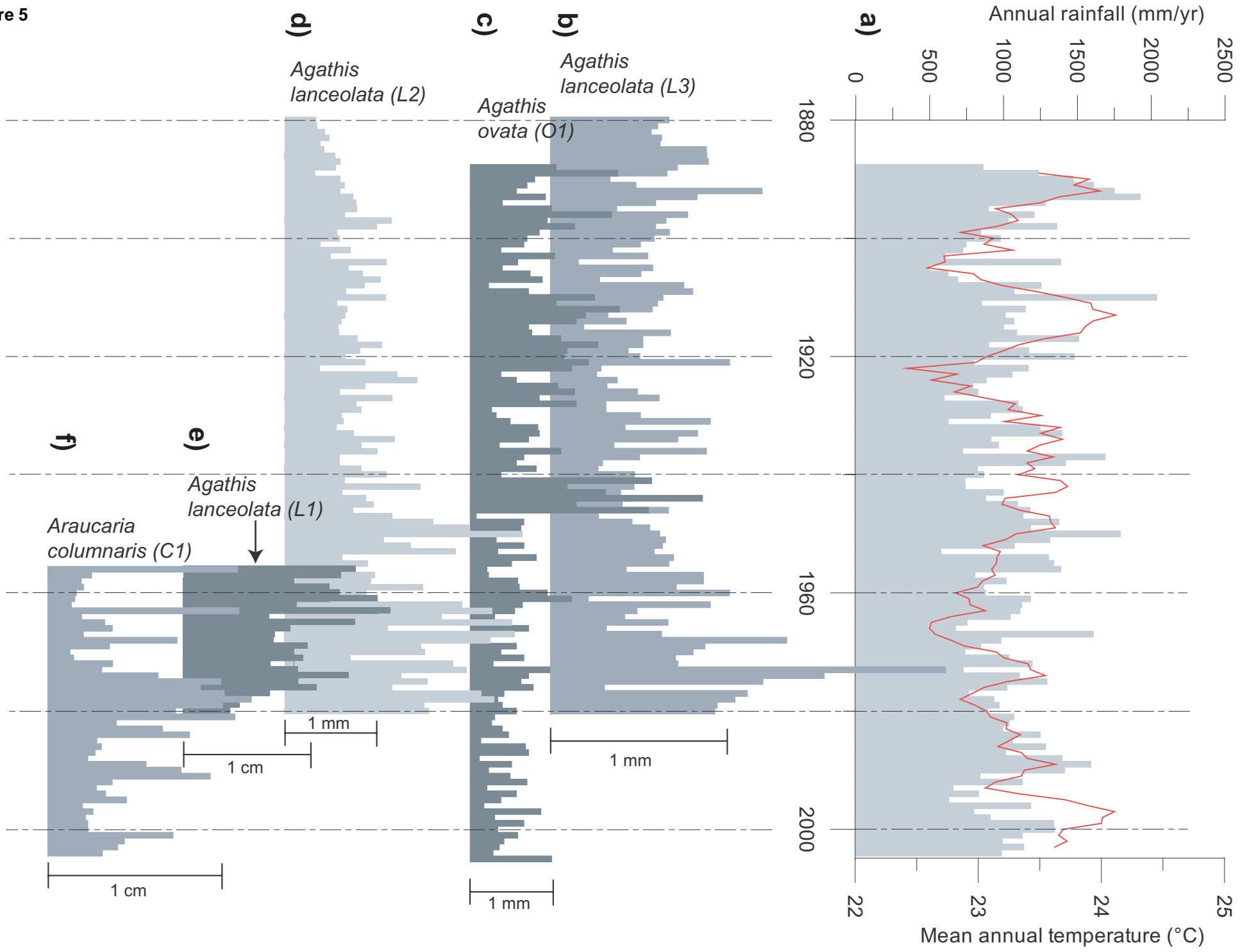


Figure 5 Lieubeau et al.

Figure 6

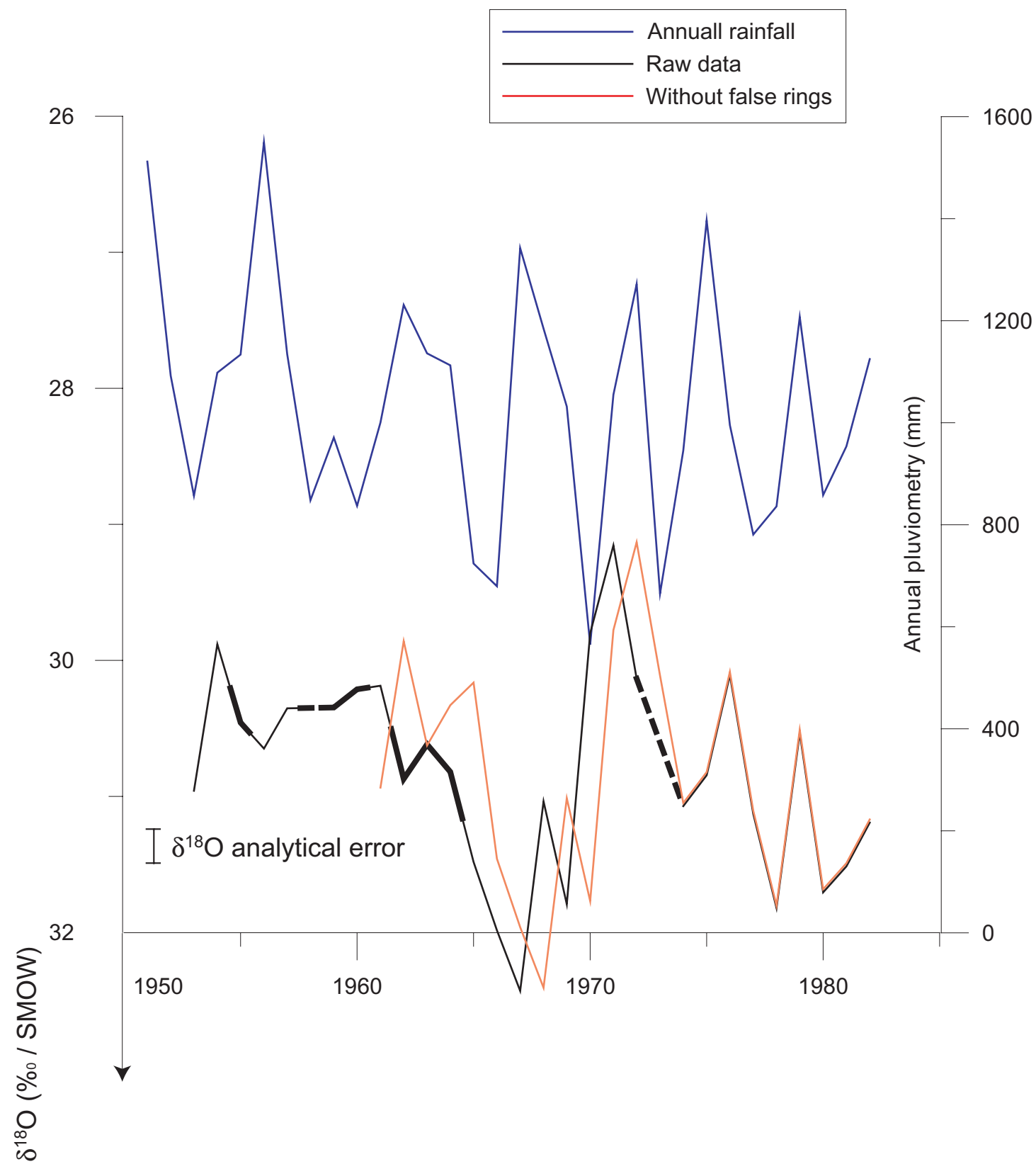


Figure 6 Lieubeau et al.